Novel Anticholinesterases Based on the Molecular Skeletons of Furobenzofuran and Methanobenzodioxepine[▽]

Weiming Luo,[†,#] Qian-sheng Yu,[†,#] Ming Zhan,[‡] Damon Parrish,[§] Jeffrey R. Deschamps,[§] Santosh S. Kulkarni,[||] Harold W. Holloway,[†] George M. Alley,[⊥] Debomoy K. Lahiri,[⊥] Arnold Brossi,[◆] and Nigel H. Greig*[,†]

Drug Design & Development Section, Laboratory of Neurosciences, and Bioinformatics Unit, Research Resources Branch, Gerontology Research Center, National Institute on Aging, National Institutes of Health, 5600 Nathan Shock Drive, Baltimore, Maryland 21224, Laboratory for the Structure of Matter, Department of the Navy, Naval Research Laboratory, Washington, D.C. 20375, Medicinal Chemistry Section, Intramural Research Program, National Institute on Drug Abuse, National Institutes of Health, 5500 Nathan Shock Drive, Baltimore, Maryland 21224, Indiana University School of Medicine, Indianapolis, Indiana 46202, and School of Pharmacy, University of North Carolina at Chapel Hill, North Carolina 27599-7361.

Received August 20, 2004

Reductive cyclization of 5-hydroxy-3-methyl-3-methoxycarbonylmethylenebenzofuran-2(3*H*)-one (**4**) gave 5-hydroxy-3a-methyl-2,3,3a,8a-tatrahydrofuro[2,3-*b*]benzofuran (**5**) and the rearrangement product 7-hydroxy-4,5-dihydro-2,5-methano-1,3-benzodioxepine (**6**). Reaction of compounds **5** and **6** with different isocyanates provided two series novel carbamates (**7**−**12**) whose structures were confirmed by X-ray crystallography. These were assessed for anticholinesterase action against freshly prepared human enzyme and proved to be potent inhibitors of either acetyl- (AChE) or butyrylcholinesterase (BChE) with specific compounds exhibiting remarkable selectivity. Because the two series of carbamates (**7**−**12**) differ in their phenolic moieties, their respective potency and selectivity for AChE versus BChE was governed by their N-substituted groups. This same characteristic was also present in a series of physovenine analogues (**1**, **13**, **15**, **17**) and physostigmine analogues (**2**, **14**, **16**, **18**). These structure−activity relations proved valuable in elucidating the mechanisms underpinning the interaction between carbamate-based cholinesterase inhibitors and their enzyme target. In addition, because physostigmine analogues have demonstrated activity in lowering the Alzheimer's disease protein, amyloid precursor protein (APP), examples of the two new series of carbamates were characterized in culture assays of quantifying cell viability and synthesis of APP.

Introduction

Physovenine (**1**), with an ether linkage in ring-C of natural physostigmine (**2**) instead of a *N*-Me group (Figure 1), is an alkaloid present in *Physostigma venenosum* whose chemistry and biological properties have been extensively reviewed.[1] The almost identical properties of **1** and **2** in inhibiting human AChE and BChE[2,3] aroused our interest in further exploring the mechanisms underpinning the action of physostigmine (**2**) and its analogues toward the discovery of potent and novel anticholinesterase because this class of compounds represents the backbone of current Alzheimer's disease (AD) treatment.[4]

Physostigmine (**2**) has served as a template in the development of several agents for AD, including a slow-release formulation of the parent compound (synapton, Forest Laboratories, St Louis, MO), its heptylcarbamate (eptylstigmine, Mediolanum, Italy), both withdrawn from clinical development because of efficacy and toxicity issues, and its phenylcarbamate (phenserine, National Institute on Aging, Baltimore, MD, and Axonyx, New York, NY) that currently is in phase 3 clinical assessment in mild to moderately afflicted patients. The pharmacodynamics that underscores the action of this class of drugs is the elevation of brain acetylcholine (ACh) levels that is achieved by inhibition of its hydrolyzing enzymes, AChE and BChE.[4] A hallmark of AD is synaptic loss, particularly of the forebrain cholinergic system that is pivotal in higher brain functions associated with learning, memory, and behavior.[4]

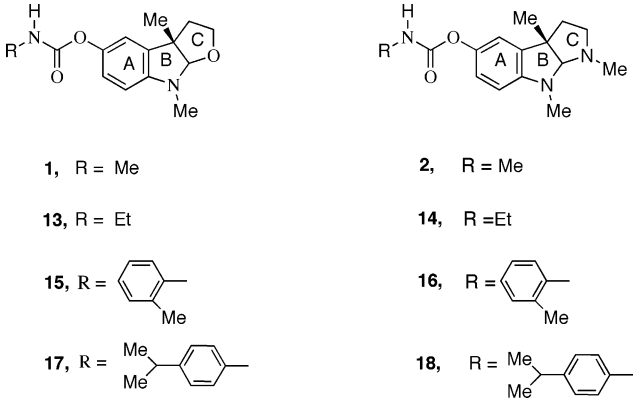

Figure 1. Chemical structures of physovenine (**1**) and physostigmine (**2**) based carbamates.

[▽] Historically known occasionally as furochroman.

* To whom correspondence should be addressed. Phone: 410-558-8278. Fax: 410-558-8323. E-mail: Greign@grc.nia.nih.gov.
[†] Laboratory of Neurosciences, National Institute on Aging.
[#] Equal contribution and joint first authorship by Drs. Weiming Luo and Qian-sheng Yu.
[‡] Gerontology Research Center, National Institute on Aging.
[§] Naval Research Laboratory.
[||] National Institute on Drug Abuse.
[⊥] Indiana University School of Medicine.
[◆] University of North Carolina at Chapel Hill.

10.1021/jm049309+ CCC: $30.25
Published on Web 01/12/2005

Extensive structural information is available on the interaction of AChE and BChE with ACh and related substrates because of extensive X-ray crystallography and mutagenesis studies.[5−7] The catalytic subunit of both enzymes has a molecular mass of 60−80 kDa, depending on its level of glycosylation and the species from which it is derived.[6] The active site for ACh hydrolysis is buried within a primarily hydrophobic 20 Å deep gorge.[7] In its interaction and inhibition of AChE and BChE, it is generally believed that under physiological conditions the basic $N^1(CH_3)$ group of physostigmine ($pK_a = 8.46$)[8] and analogues gains a H^+ to form a quaternary ammonium group. In a manner similar to ACh, positively charged physostigmine is drawn into the enzyme by electrostatic field forces. Thereafter, it interacts with specific binding domains to form an inhibitor−enzyme complex. Whereas the quaternary ammonium group plays an important role in this process, physovenine (**1**), which bears a neutral ring-C oxygen instead of basic ring-C nitrogen, appears to be equipotent as an anticholinesterase, as is the ring-C thia analogue of **1**, thiaphysovenine.[9]

This phenomenon can be potentially explained by the common capacity of the ether oxygen and amino nitrogen of **1** and **2** to form H-bonds with amino acids, providing the basis of the interaction between the compounds and enzyme. However, the common ring-B−$N^8(CH_3)$ in both provides a weaker basic group ($pK_a = 3.7$)[8] and hence reintroduces the potential involvement of charge into the compound−enzyme interaction. To totally exclude the possibility of forming a positively charged molecule, we synthesized analogues of **2** with the nitrogen atoms of the tricyclic moiety replaced by ether oxygen and assessed the activity of the resulting novel compounds as anticholinesterases. The resulting tetrahydrofuro[2,3-*b*]benzofuran is an important structural component of aflatoxins, mold metabolites studied extensively by Büchi,[10] Rapoport,[11] Townsend,[12] and others. However, rather than creating the tricyclic moiety by chemistry published by these authors, we started with 3-methyl-5-hydroxybenzofuran-2-one (**3**), readily available from 1,4-cyclohexandione and pyruvic acid,[13] and its further application. This is reminiscent of chemistry employed earlier by Harley-Mason in his synthesis of physostigmine (**2**).[14] We herein describe the anticholinesterase activity against human enzyme for this novel series of carbamates, and because physostigmine analogues have demonstrated activity to lower the levels of the AD protein amyloid precursor protein (APP)[15] that generates the neurotoxic peptide, Aβ[16], we assessed the action of specific examples on the cellular viability and production of secreted APP of immortal human cells in culture.

Results

Chemistry. 5-Hydroxybenzofuran-2-one (**3**) was obtained by condensation of 1,4-cyclohexandione with pyruvic acid according to published methodology.[13] The crude product, **3**, was crystallized directly from the reaction mixture without chromatography. Its recrystallization from ethanol gave pure crystalline **3** in a 40% yield. C-3 alkylation of compound **3** with methyl chloroacetate, using 1 equiv of sodium hydride as a base, gave compound **4,** which also was purified by simple crystallization without using chromatography (Scheme 1).

Scheme 1[a]

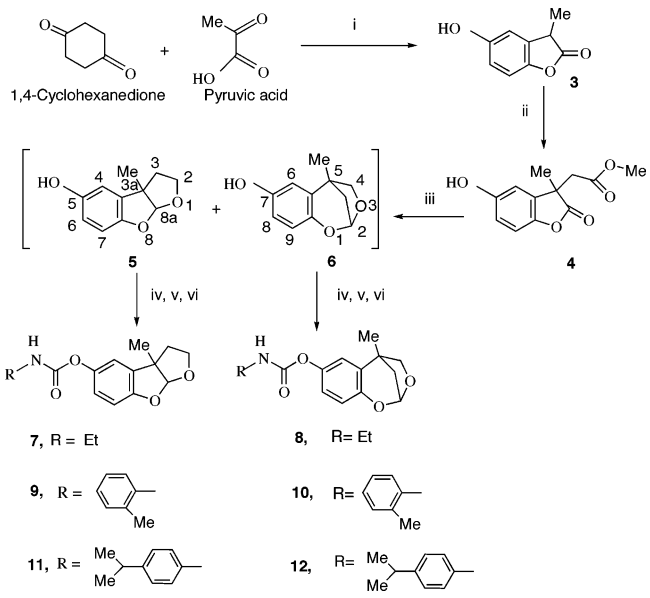

[a] Reagents: (i) 160-170 °C, 3 h; (ii) $ClCH_2COOCH_3$/DMF, NaH, 0 °C, 1 hr, then room temp, overnight; (iii) (a) LAH/THF, room temp, 1 h; (b) oxalic acid, 0.5 h; (iv) Na, EtNCO/Et_2O, room temp, 1 h; (v) Na, *o*-tolyl isocyanate/Et_2O, room temp, 0.5 h; (vi) Na, *p*-isopropylphenyl isocyanate/Et_2O, room temp, 45 min.

It has been reported that the oxindole corresponding to compound **4**, 3-methoxycarbonylmethylene oxyindole-2-one, is able to convert to physovenol.[17] On the basis of this, we conceived that compound **4** would be amenable to reductive cyclization to provide the desired tricyclic target compound **5**. Applying normal reductive conditions in practice, however, we gained a mixture of highly polar compounds. The departure of our obtained products from those predicted was likely derived from the following. First, in lieu of an amide in ring-B, as occurs in the oxyindole,[17] compound **4** has a lactone. This may be easily reduced to form tetrol, **19**, which contains both phenol and alcohol groups. After intermolecular dehydration and cyclization, **19** became a complex mixture of different products. Second, desired compound **5** is an acetal that under acidic conditions exists in an equilibrium between acetal **5** and aldehyde **20** (Scheme 2). The 1,4-hydroquinone in compound **20** is not a stable moiety, being easily oxidized to form complex products. To avoid the equilibrium moving toward the formation of aldehyde **20**, strong aqueous acid was avoided in the synthesis. Hence, after reduction of compound **4** by $LiAlH_4$ in THF at room temperature for 1 h, solid oxalic acid, rather than dilute HCl, was added to the reaction mixture as a hydrolysis reagent. This replacement provided us compound **5** together with the unexpected compound **6** in a ratio of 1:1. In the same manner as proposed for **5**, **6**, in an aqueous acidic condition, likely is in equilibrium with aldehyde **21**. The reaction mechanism remains to be fully elucidated and is a focus of current investigation.

Separation of compounds **5** and **6** by chromatography proved to be difficult because of their similar polarities. As a consequence, a mixture of **5** and **6** was reacted with different isocyanates to provide three pairs of carbamates **7** and **8**, **9** and **10**, and **11** and **12**. Each pair of compounds was separated by preparative TLC to generate the final products in high purity. In summary, this

Scheme 2

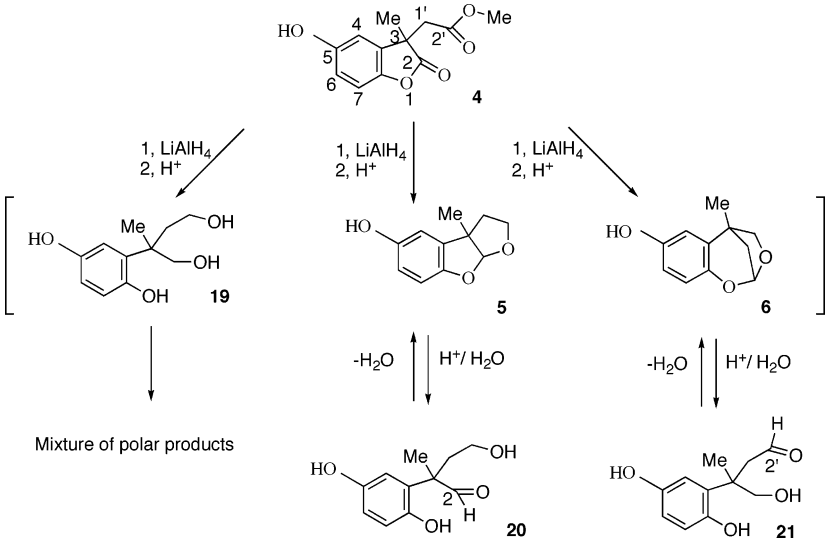

four-step total synthesis provided a simple means to obtain compounds containing the molecular skeletons of tetrahydrofurobenzofuran (**5**) and 4,5-dihydro-2,5-methano-1,3-benzodioxepine (**6**). The reductive cyclization of compound **4** requires additional optimization to generate a higher yield.

Because this represents the first description of these types of carbamates and the intromolecular rearrangement that occurs during the reductive cyclization of compound **4**, the structures of **7**−**12** were characterized not only by routine MS, ^{1}H NMR and ^{13}C NMR but additionally by ^{1}H NMR COSY 45. The latter proved useful in defining the bridged structure of compound **8**. Specifically, a correlation between bridged methylene C10−H_2 (δ 2.19−1.91 ppm) and the C2−H (δ 5.69) on the bridgehead position was present in **8** and contrasts with the C8a−H (δ5.77 ppm) of **7**, where there is no correlation of methylenes, C2−H_2 (4.06−3.56 ppm) and C3−H_2 (2.13−1.91 ppm) (see Supporting Information). Finally, single crystals of **11** and **12** were obtained and analyzed by X-ray crystallography to confirm their structures (Figure 2).

For comparison, the ethylcarbamate of physovenol (**13**) was synthesized using a published method.[3] The ethylcarbamate of eseroline (**14**) was also synthesized according to known procedure.[15]

X-ray Crystallography. The results of the X-ray studies are illustrated in Figure 2.

For compound **11**, the four atoms of the carbamoyl moiety −N−CO−O− compose a plane. The angle between planes *N*-phenyl and carbamoyl is 10.95°. The angle between the carbamoyl and *O*-phenyl (ring-A) is 95.75°. These two aromatic rings are almost perpendicular to each other (84.80°). The terminal five-membered ring-C has an envelope conformation with C3 being out of plane atoms. The central five-membered ring-B is coplanar with its adjoining phenyl ring. The fused ring system is folded at the bond in common with the two five-membered rings (C3a−C8a). The angle of O8−C8a−O1 is 108.32°.

For compound **12**, the four atoms of carbamoyl −N−CO−O− also are in a plane. The angle between planes *N*-phenyl and carbamoyl is 4.33°. The angle between carbamoyl and *O*-phenyl (ring-A) is 72.27°. The *N*-phenyl ring is at 67.94° to the *O*-phenyl (ring-A). The 1,3-dioxepine is folded at the bridgehead C2−C5. The angle of C10−C2−O1 is 113.17°, the angle of C10−C2−O3 is 117.8°, and the angle of O1−C2−O3 is 108.68°.

Biological Evaluation. Table 1 illustrates the biological activity of compounds **7**−**12** against freshly prepared human AChE and BChE, in comparison to the corresponding carbamates of physovenol (**1**, **13**, **15**, **16**) and eseroline (**2**, **14**, **17**, **18**), whose measured values were similarly obtained.[18] Because we have previously demonstrated that physostigmine analogues with straight-chain *N*-alkyl (e.g., methyl, butyl, and octyl)

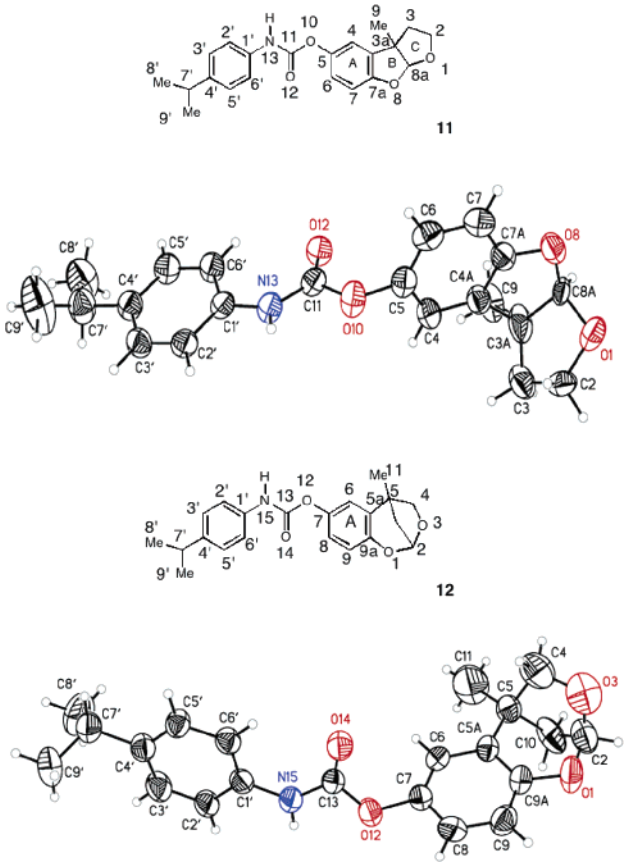

Figure 2. X-ray crystallographic picture and corresponding chemical structures of **11** and **12**.

Table 1. 50% Inhibitory Concentration of Compounds versus Human Erythrocyte AChE and Plasma BChEIC_{50}

	compound	IC_{50} ± SEM (nM) AChE	BChE	selectivity
	Physovenine Series[a]			
1	(−)-methylcarbamate	27 ± 1	4 ± 1	7-fold BChE
13	(−)-ethylcarbamate	82± 4	2 ± 0.1	40-fold BChE
15	(−)-2′-methylphenylcarbamate	13 ± 1	1560 ± 120	120-fold AChE
17	(−)-4′-isopropylphenylcarbamate	3860 ± 970	17 ± 2	227-fold BChE
	Physostigmine Series[a]			
2	(−)-methylcarbamate	28 ± 2	16 ± 3	2-fold BChE
14	(−)-ethylcarbamate	94 ± 12	4 ± 0.1	23-fold BChE
16	(−)-2′-methylphenylcarbamate	10 ± 2	1950 ± 240	195-fold AChE
18	(−)-4′-isopropylphenylcarbamate	760 ± 20	50 ± 1	15-fold BChE
	Tetrahydrofurobenzofuran Series			
7	(±)-ethylcarbamate	360 ± 22	6 ± 2	60-fold BChE
9	(±)-2′-methylphenylcarbamate	23 ± 4	>30,000	>1300-fold AChE
11	(±)-4′-isopropylphenyl carbamate	2650 ± 400	27 ± 4	100-fold BChE
	Dihydrobenzodioxepine Series			
8	(±)-ethylcarbamate	830 ± 86	24 ± 5	35-fold BChE
10	(±)-2′-methylphenylcarbamate	56 ± 1	>30000	>535-fold AChE
12	(±)-4′-isopropylphenylcarbamate	4300 ± 350	22 ± 5	195-fold BChE

[a] The IC_{50} data of compounds **1**, **2**, **15**, **16**, **18** are from ref 14, and the data of compound **17** are from ref 3. Examples of these were reanalyzed and closely matched the provided values.

Table 2. Comparison of the IC_{50} Values of Anticholinesterases of Clinical Interest against Human Erythrocyte AChE and Plasma BChE

compound	IC_{50} [a] ± SEM (nM) AChE	BChE	selectivity
tacrine (cognex)	190 ± 40	47.0 ± 10	4-fold BChE
donepezil (aricept)	22 ± 8	4150 ± 1700	188-fold AChE
galanthamine (reminyl)	800 ± 60	7300 ± 830	9-fold AChE
rivastigmine (exelon)	4150 ± 160[b]	37 ± 5	122-fold BChE
phenserine	22 ± 1.4	1560 ± 45	70-fold AChE
2′-ethylphenylgeneserine *N*-oxide HCL (CHF2819)	125 ± 23	1700 ± 385	14-fold AChE
heptylphysostigmine (eptastigmine)	22 ± 2	5.0 ± 0.1	4-fold BChE
huperzine A	47 ± 22	>10000	>212-fold AChE

[a] IC_{50} values were determined in duplicate on a minimum of four different occasions. [b] Rivastigmine is atypical in that its activity against brain-derived AChE is far more potent than against red blood cell derived enzyme.[40] The measured value may therefore noticeably underestimate its activity in brain, and the agent has been reported to be nonselective between AChE and BChE.

carbamoyl moieties have similar anticholinesterase activities,[19−21] we synthesized the *N*-ethylcarbamates (**7**, **8**, **13**, and **14**) as the representative of this class. Ethyl isocyanate is commercially available and safer than the methyl analogue for transport and handling. All compounds (**7**−**12**) are racemic.

Tetrahydrofurobenzofuran Series. The tetrahydrofurobenzofuran carbamates (**7**, **9**, **11**) proved to be potent anticholinesterases. Like physovenine (**1**), the ethylcarbamate (**7**) possessed potent BChE inhibitory action but surprisingly low AChE activity to provide it a BChE selectivity of 60-fold. The 2′-methylphenylcarbamate, which for both the physostigmine and physovenine series (**16**, **15**) provided AChE potency and selectivity, similarly provided the tetrahydrofurobenzofuran series (**9**) with high AChE potency. Interestingly, the compound was devoid of BChE action at the highest concentration assessed, 30 μM, providing it a remarkable and unexpected AChE selectivity. In contrast, the 4′-isopropylphenylcarbamate, which for both the physostigmine and physovenine series (**18**, **17**) reverses the potency and selectivity to favor BChE, correspondingly provided the tetrahydrofurobenzofuran series (**11**) a high BChE potency.

Dihydrobenzodioxepine Series. The dihydrobenzodioxepine carbamates (**8**, **10**, **12**) mirrored the selectivity described for the tetrahydrofurobenzofurans but with slightly less potency. This potency was favorable in comparison to many of the clinically available anticholinesterases (Table 2), and the enzyme subtype selectivities achieved by **10** and **12** were superior to those of the more classical physostigmine series.

Actions on Cellular Viability and Toxicity and Secretion of Amyloid-β Precursor Protein Levels in a Neuronal Cell Line. Because phenserine has demonstrated the ability to lower APP, the precursor to the putative Alzheimer toxin amyloid-β peptide (Aβ) in neuronal cell lines,[15] representative carbamates **9** and **10** were assessed for actions on APP in human neuroblastoma SK-N-SH cells in culture. Cell viability and toxicity were additionally quantified by MTT assay and measurement of lactate dehydrogenase levels, respectively, at 48 h. Neither compound altered secreted levels of APP at the concentrations assessed (10 and 30 μM), which were well tolerated. As illustrated in Figure 3, however, there was a significant increase in cell viability induced by **10** at the lower concentration. This was validated by quantifying viable cell number by trypan blue cell count (Figure 3).

Discussion

Novel Potent AChE and BChE Inhibitors. Our previous studies have demonstrated that phenylcarbamates in the physostigmine series are long-acting and well-tolerated cholinesterases inhibitors, with a selectivity for AChE or BChE that depends on the position of

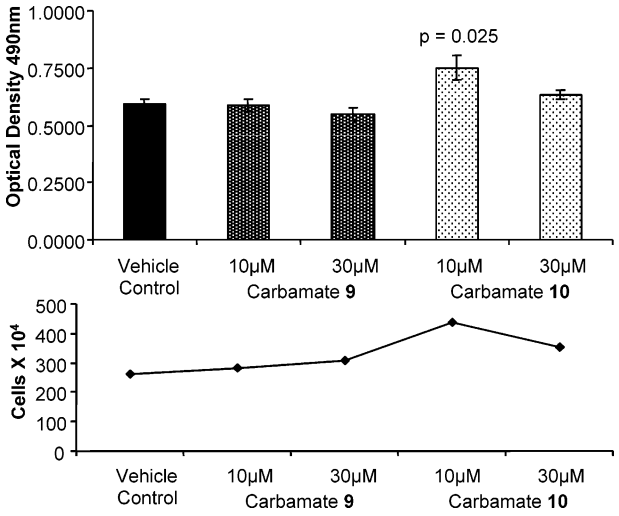

Figure 3. Action of carbamates **9** and **10** on cell viability (upper) as assessed by MTT assay and cell number (lower) as assessed by trypan blue cell count (mean ± standard error of the mean). **10** significantly elevated cell viability and cell count (Dunnett's *t*-test).

phenyl ring substitution.[22,23] In this regard, the experimental drug phenserine and it 2′-substituted analogue, tolserine (**16**), have demonstrated safety and efficacy in clinical and preclinical studies, respectively.[22] On the basis of the same pharmacophore, the described novel tetrohydrofurobenzofuran (**7**, **9**, **11**) and dihydrobenzodioxepine (**8**, **10**, **12**) carbamates possess potent and clinically relevant activity (Tables 1 and 2). This is combined with unexpectedly high enzyme subtype selectivity for the substituted phenylcarbamates from both series and an economy of synthesis for the racemic compounds that makes them highly attractive agents for further development as drug candidates.

Enzyme−Inhibitor Binding Interactions. On the basis of extensive X-ray crystallography and mutagenesis studies, AChE appears to have three binding domains that interact separately or in a combined manner with divergent enzyme inhibitors.[24,25] Their binding affinities are dependent, in part, on their three-dimensional fit within the substrate gorge of the enzyme, alignment with one or more of the binding domains, and the chemical basis underpinning the interaction between inhibitor and binding domain.[23] Physostigmine analogues access the same two binding domains as does the natural substrate ACh.[6]

Table 1 illustrates that the potency and AChE versus BChE selectivity of the four series of carbamates depend on the N-substituted group of the carbamoyl moiety. Specifically, the *N*-alkyl and *N*-4′-isopropylphenylcarbamates are BChE-selective, whereas the *N*-2′-methylphenylcarbamate is AChE-selective, irrespective of the phenol: physovenines (**1**, **13**, **15**, **17**), physostigmines (**2**, **14**, **16**, **18**), tetrahydrofurobenzofuran (**7**, **9**, **11**), or bridged benzodioxepine (**8**, **10**, **12**). This is illustrated in Figure 4 in which the four AChE active compounds, **15**, **16**, **9** (in a 3a-*S* configuration), and **10** (in a 5-*S* configuration), are superimposed in an optimized conformation.

The carbamoyl moieties perfectly overlap, suggesting a similar inhibitory mechanism and in accord with similar inhibitory activities, but slight deviations exist in the overlay of the phenols. Specifically the N^1-methyl

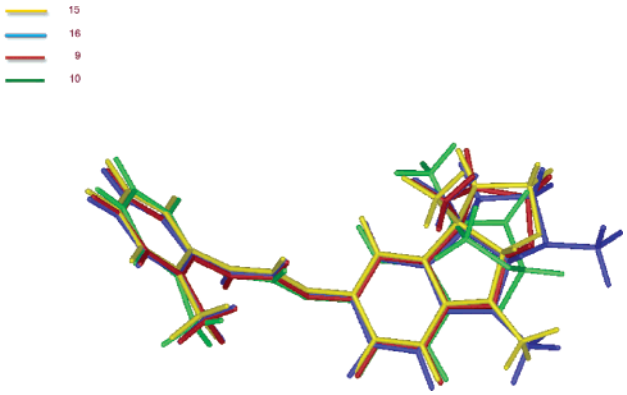

Figure 4. Superimpositon of compounds **15**, **16**, **9**, and **10**.

group of tolserine (**16**) protrudes away from the rest. This may explain the enantiomeric selectivity found with the physostigmine series, with the (+)-enantiomers being cholinergically inactive, whereas both enantiomers are active for the physosvenine as well as N^1-norphysostigmine series.[3,23,26] Because the two novel racemic carbamates (**7**−**12**) lack a N^1-methyl group but are potent anticholinesterases, we predict that their enantiomeric selectivities should be lower than those of (−)-physostigmine (**2**) and analogues. Synthesis of optically pure enantiomers is ongoing to test this hypothesis.

Chemical Interactions underpinning Activity. The kinetic analysis of cationic ligands has shown that the active site of AChE has a large negative charge,[27] thus creating a strong dipole along the active site gorge.[28] An electronic steering mechanism has been proposed for ligand binding.[29] However, the crystal structure of AChE from *Torpedo californica* has shown high aromatic content of the active site, suggesting an aromatic guidance mechanism for ligand binding.[7] The novel tetrahydrofurobenzofuran (**7**, **9**, **11**) and dihydrobenzodioxepine (**8**, **10**, **12**) carbamates, unlike physostigmine (**2**), lack a ring-C amino group to capture a proton and bear a positive charge. Thus, this novel set of compounds has a different dipole moment and vector of the dipole than does physostigmine and related carbamates.

To assess H-bonding and other binding interaction between these compounds and AChE, compound **9** and *Torpedo californica* AChE (TcAChE, EC 3.1.1.7.) was modeled (Figure 5). Specifically, the crystal structure of TcAChE, carbamoylated by the physostigmine analogue, 8-(*cis*-2,6-dimethylmorpholino)octyleseroline (MF 268), was utilized for this purpose.[30] The carbamoyl moiety was removed from this complex to allow compound **9** to be docked in the active site of AChE (Figure 5).

As illustrated and similar to studies of ACh,[5,31] the carbonyl group of compound **9** is in the vicinity of the "oxyanion hole", the backbone N−H of Gly 118, Gly 119, and Ala 201. The carbamate N−H interacts with the His 440 of the catalytic triad (Figure 5). With two points (N−H and C=O) fixed to the backbone of the binding domain, the degree of freedom of the *N*-phenyl group is tremendously decreased. In summary, this part of each compound is relatively fixed and tolerates little structural change without a loss of binding and resulting inhibitory action.

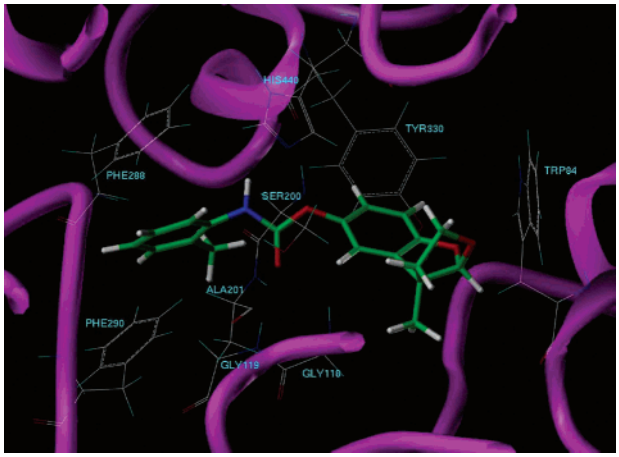

Figure 5. Docking model of compound **9** in the binding domain of AChE. The amino acid residues are numbered on the basis of the *T. Californica* sequence.

The noncationic tricyclic phenol portion is oriented in the "anionic" site, lined with hydrophobic residues, Trp 84 and Tyr 330, gaining the binding energy by hydrophobic interactions. Recently, a X-ray crystal of a neutral molecule within AChE demonstrated the binding of a noncationic group within the anionic site, with cation−π mimicking C−H···π interactions.[32] This indicates that the structural modification of our tricyclic structure can be tolerated and will allow specific interactions to differentiate the four series of analogues.[23,33] The *o*-tolyl group of compound **9** binds in the active site gorge near the hydrophobic residues Phe 288 and Phe 290, forming stacking interactions. These residues have been implicated for the substrate selectivity of AChE and BChE,[24,25] thus explaining the observed selectivity of the compound **9** toward AChE.

The new dioxygen compounds **7**−**12** are, in reality, spiroacetals. As such, they can be more readily hydrolyzed by acid than can ethers but are extremely resistant to hydrolysis by bases. Their described ex vivo biological evaluation was undertaken in a pH 8.0 buffer because this represents the optimal working environment for AChE and BChE.[6,20,22−24] Hence, compounds **7**−**12** are predicted to be stable prior to interacting with either cholinesterase enzyme. Their similar anticholinesterase activities and selectivities compared to those of other tricyclic compounds, as exemplified by the physovenine and physostigmine series (Table 1), support this hypothesis. However, as spiroacetals, they may be more supportive of a hydrogen-bonding interaction within the enzyme. If this occurred, such interaction could potentially lead to a charge delocalization through the acetal moiety, a greater ease of protonation of one of the acetal oxygens, and hydrolysis of the acetal system to form ring open compounds. Thus, the character of the spiroacetal may represent a fruitful area for further characterization in future studies.

Action on Cellular Viability and Amyloid-β Precursor Protein Levels. Human SK-N-SH cells in culture express cholinergic markers, synthesize and secrete APP, and have proven to be useful in defining the action of experimental compounds on AD amyloidogeneis.[15,16] In contrast to (−)-phenserine (10 and 30 μM), which lowers secreted APP levels by 50%,[15] **9** and **10** lacked APP action. Such action for (−)-phenserine, however, is not cholinergically mediated because its (+)-enantiomer, which lacks anticholinesterase activity, lowers APP and, as a consequence, Aβ levels.[15] Furthermore, the inhibition of cholinergically mediated biochemical pathways, specifically those involving MAP kinase and PI kinase (whose activation are associated with anticholinesterase action and muscarinic receptor stimulation[16] without the loss of action on APP) confirmed the disassociation between phenserine's action as an anticholinesterase and as an APP inhibitor.[15] The APP lowering activity appears to be post-transcriptionally mediated via the 5′-untranslated region of APP mRNA[15] through a specific region containing a CAGA box that is conserved in mammals that deposit Aβ[34]. Like **9** and **10**, (−)-physotigmine (**2**) also lacks this APP action,[35] and the structure−activity relationship underpinning it is the focus of ongoing studies.

In contrast, we have never previously observed an increase in cell viability, as induced by **10**, despite the fact that we routinely perform MTT assays to discriminate between drug-induced biochemical changes and toxicity. The mechanism underpinning this activity is being investigated, and because neither **2** nor prior carbamates have demonstrated this action, it likely is noncholinergically mediated.

In summary, we have synthesized and characterized novel tetrahydrofurobenzofuran (**7**, **9**, **11**) and dihydrobenzodioxepine (**8**, **10**, **12**) carbamates that possess potent and clinically relevant anticholinesterase activity. These compounds not only are interesting candidates as experimental agents for AD, head trauma, glaucoma, and nerve gas prophylaxis, for which anticholinesterases have previously demonstrated clinical utility, but have proven valuable as tools to characterize the molecular interactions that underpin the classic cholinesterase inhibitory action of (−)-physostigmine (**2**), its ring-B and ring-C congeners, and their clinically relevant carbamates.

Experimental Section

Chemistry. Melting points (uncorrected) were measured with a Fisher-Johns apparatus. ^{1}H NMR and ^{13}C NMR were recorded on a Bruker (Bellevica, MA) AC-300 spectrometer. MS (*m/z*) data were recorded on a Hewlett-Packard 5973 GC−MS (CI). HRMS experiments were performed by the UCR Mass Spectrometry Facility, Department of Chemistry, University of California. All reactions involving nonaqueous solutions were performed under an inert atmosphere.

(−)-(3a*S*)-3a,8-Dimethyl-2,3,3a,8a-tetrahydrofuro[2,3-*b*]indol-5-yl *N*-Ethylcarbamate (13). It was made according to a known procedure[3] for making (−)-physovenine. In this case, the mole ratio (physovenol/ethyl isocyanate) was 1:3 and the reaction time was increased to about 3 h (monitored by TLC). The product was obtained quantitatively as a gum: [α] -97.4° (*c* 0.2, $CHCl_3$); ^{1}H NMR ($CDCl_3$) δ 6.77 (m, 2H, C4−H and C6−H), 6.22 (d,1H, C7−H), 5.10 (s, 1H, C8a−H), 4.85 (s, br, 1H, N−H), 3.90 (m, 1H, C2−H_a), 3.40 (m, 1H, C2−H_b), 3.30 (q, 2H, $-CH_2-$), 2.88 (s, 3H, N^8-CH_3), 2.00 (m, 2H, C3−H_2), 1.40 (s, 3H, C3a−CH_3), 1.20 (t, 3H, $-CH_3$); CI-MS (CH_4), *m/z* 277 (MH^+). HR-MS *m/z* calcd for $C_{15}H_{21}N_2O_3$: 277.1552. Found: 277.1563. Anal. ($C_{15}H_{20}N_2O_3 \cdot {}^1/_4H_2O$) C, H, N.

(−)-(3a*S*)-1,3a,8-Trimethyl-1,2,3,3a,8,8a-hexahydropyrrolo[2,3,*b*]indol-5-yl *N*-Ethylcarbamate (14). It was made according to a known procedure[19] by using ethyl isocyanate as alkyl isocyanate. The product was obtained quantitatively as crystals: mp 92−93 °C; [α] −60.9° (*c* 0.1, $CHCl_3$); ^{1}H NMR ($CDCl_3$) δ 6.72 (m, 2H, C4−H and C6−H), 6.29 (d, 1H, C7−H), 4.85 (s, br, 1H, N−H), 4.10 (s, 1H, C8a−H), 3.00

(q, 2H, $-CH_2-$), 2.90 (s, 3H, N^8-CH_3), 2.60 (m, 2H, C2−H_2), 2.52 (s, 3H, N^1-CH_3), 1.90 (m, 2H, C3−H_2), 1.45 (s, 3H, C3a−CH_3), 1.20 (t, 3H, $-CH_3$); CI-MS (CH_4), *m/z* 290 (MH^+). HR-MS *m/z* calcd for $C_{16}H_{24}N_3O_2$: 290.1869. Found: 290.1865. Anal. ($C_{16}H_{23}N_3O_2$) C, H, N.

5-Hydroxy-3-methylbenzofuran-2(3*H*)-one (3). Pyruvic acid (8.81 g, 0.10 mol) was added to 1,4-cyclohexanedione (11.2 g, 0.10 mol). The reaction mixture was heated to 160−170 °C and then stirred for 3 h. The mixture was maintained at room temperature to allow crystallization. Filtration gave a crude product that then was recrystallized from ethanol to provide product **3** as pale-yellow crystals (6.50 g, 40%): mp 172.0−173.0 °C; ^{1}H NMR ($CDCl_3$) δ 6.80−6.51 (m, 3 H, Ph−H), 4.69 (s, 1H, OH), 3.55 (q, 1H, C3−H), and 1.38 (d, 3H, C3−CH_3) ppm; CI-MS (CH_4), *m/z* 165 (MH^+) and 137.

5-Hydroxy-3-methyl-3-methoxycarbonylmethylenebenzofuran-2(3*H*)-one (4). Under a nitrogen atmosphere, sodium hydride (0.24 g, 0.01 mol) was added to a solution of compound **3** (1.64 g, 0.01 mol) and methyl chloroacetate (1.19 g, 0.01mol) in 6 mL of dry DMF at 0 °C in portions over 1 h. The mixture was stirred for another hour at 0 °C and then overnight at room temperature. The reaction mixture was poured over 25 g of ice and extracted with ether (20 mL × 3). The extracted solution thereafter was washed with brine (20 mL × 2) and dried over magnesium sulfate. The final concentrated solution was maintained at room temperature and crystallized to provide a crude product that then was recrystallized from EtOAc to give product **4** as white needlelike crystals (1.09 g, 46.1%): mp 153.5−155.0 °C; ^{1}H NMR ($CDCl_3$) δ 6.92−6.61 (m, 3 H, Ph−H), 5.07 (s, 1H, OH), 3.44 (s, 3H, OCH_3), 3.02, 2.84 (AB, J_{gem} = 18.0 Hz, 2H, C3−CH_2CO), and 1.41 (s, 3H, C3−CH_3) ppm; ^{13}C NMR ($CDCl_3$) δ 179.7, 170.0, 154.0, 144.9, 132.1, 114.6, 110.6, 110.2, 51.5, 44.5, 40.9, and 24.7 ppm; CI-MS (CH_4), *m/z* 237 (MH^+), 205, and 177; HR-MS *m/z* calcd for $C_{12}H_{12}O_5$: 236.0685. Found: 236.0673.

5-Hydroxy-3a-methyl-2,3,3a,8a-tatrahydrofuro[2,3-*b*]-benzofuran (5) and 7-Hydroxy-4,5-dihydro-2,5-methano-5-methyl-1,3-benzodioxepine (6). Under a nitrogen atmosphere, a solution of compound **4** (1.04 g, 4.40 mmol) in 20 mL of THF was added dropwise to lithium aluminum hydride (0.33 g, 8.70 mmol) in THF (20 mL) at room temperature. The mixture was stirred for 1 h at room temperature, and then oxalic acid (1.97 g, 21.90 mmol) was added and the mixture was stirred for another 0.5 h at room temperature. The mixture was filtered, and a solid material was partitioned between the ether and aqueous solution of oxalic acid. Thereafter, the combined THF and ether solution was evaporated to remove solvents. The resulting residue was chromatographed on silica gel (EtOAc/hexane = 1/3) to provide a mixture of **5** and **6** as a gum (84.8 mg, 10.0%): ^{1}H NMR ($CDCl_3$) δ 6.75−6.60 (m, 6 H, Ph−H), 5.85 (s, 1H, C8a−H of **5**), 5.78(d, J = 1.80 Hz, 1H, C2−H of **6**), 1.55 (s, 3H, C3a−CH_3 of **5**), 1.50 (s, 3H, C5−CH_3 of **6**) ppm; GC−MS (CI): two peaks (1:1), *m/z* 193 (MH^+), respectively. It was directly used as a reactant in the following reactions without separation.

3a-Methyl-2,3,3a,8a-tetrahydrofuro[2,3-*b*]benzofuran-5-yl *N*-Ethylcarbamate (7) and 4,5-Dihydro-2,5-methano-5-methyl-1,3-benzodioxepin-7-yl *N*-Ethylcarbamate (8). Under a nitrogen atmosphere, two small pieces of sodium (∼1 mg per piece) were added to a solution of compounds **5** and **6** (32.0 mg, 0.166 mmol) in 5 mL of dry ether at room temperature. The mixture was stirred for 2 min, and then ethyl isocyanate (24.8 mg, 0.349 mmol) was added in one portion. The reaction was continued for another 1 h at room temperature, then 5 mL of water was added, and the ether layer was separated. After the sample was dried over sodium sulfate and filtered, the filtrate was evaporated to provide a residue that then was chromatographed (preparative TLC, silica gel, EtOAc/hexane = 1/3). This latter procedure was repeated on three occasions to afford products **7** (11.3 mg, 51.7%) and **8** (13.2 mg, 60.4%) as colorless gums.

Product 7: ^{1}H NMR ($CDCl_3$) δ 6.87−6.60 (m, 3H, Ar−H), 5.77 (s, 1H, C8a−H), 4.89 (s, br, 1H, NH), 4.06−3.56 (m, 2H, C2−H), 3.23 (q, 2H, CH_2 of EtNH−), 2.13−1.91 (m, 2H, C3−H), 1.47 (s, 3H, C3a−CH_3), and 1.14 (t, 3H, CH_3 of EtNH−) ppm; ^{13}C NMR ($CDCl_3$) δ 155.2, 153.9, 144.4, 131.9, 120.6, 115.9, 115.8, 108.4, 67.6, 52.9, 40.1, 35.1, 23.2, and 14.1 ppm; CI-MS (CH_4), *m/z* 264 (MH^+), 193, 175, and 72; HR-MS *m/z* calcd for $C_{14}H_{17}NO_4$: 263.1158. Found: 263.1162. Anal. ($C_{14}H_{17}N\ O_4$) C, H, N.

Product 8: ^{1}H NMR ($CDCl_3$) δ 6.82−6.67 (m, 3H, Ar−H), 5.69 (d, J = 1.80 Hz, 1H, C2−H), 4.88 (s, br, 1H, −NH−), 4.17, 3.70 (AB, J_{gem} = 7.20 Hz, 2H, C4−H_2), 3.22 (q, 2H, CH_2 of EtNH−), 2.19−1.91 (m, 2H, C10−H_2), 1.41 (s, 3H, C5−CH_3), and 1.16 (t, 3H, CH_3 of EtNH−) ppm; ^{13}C NMR ($CDCl_3$) δ 155.3, 149.3, 145.0, 132.7, 121.7, 117.3, 117.0, 100.8, 84.8, 40.0, 36.5, 21.1, 17.2, and 15.5 ppm; CI-MS (CH_4), *m/z* 264 (MH^+), 246, 220, 193, 175, 149, and 72. HR-MS *m/z* calcd for $C_{14}H_{17}NO_4$: 263.1158. Found: 263.1164. Anal. ($C_{14}H_{17}N\ O_4 \cdot {}^1/_8H_2O$) C, H, N.

3a-Methyl-2,3,3a,8a-tetrahydrofuro[2,3-*b*]benzofuran-5yl *N*-(2′-Methylphenyl)carbamate (9) and 4,5-Dihydro-2,5-methano-5-methyl-1,3-benzodioxepin-7-yl *N*-(2′-Methylphenyl)carbamate (10). Under a nitrogen atmosphere, two small pieces of sodium (∼1 mg per piece) were added to a solution of **5** and **6** (29.5 mg, 0.153 mmol) in 5 mL of anhydrous ether at room temperature. The mixture was stirred for 2 min, and then *o*-tolyl isocyanate (20.4 mg, 0.153 mmol) was added in one portion. The reaction was continued for 30 min at room temperature. Thereafter, 5 mL of water was added and the ether layer was separated. After the sample was dried over sodium sulfate and filtered, solvent was removed from the filtrate by evaporation. The residue was chromatographed on a preparative TLC silica gel plate (EtOAc/hexane = 1/3) to afford products **9** (18.6 mg, 74.9%) and **10** (16.1 mg, 64.4%) as a colorless gum.

Product 9: ^{1}H NMR ($CDCl_3$) δ 7.84 (s, br, 1H, −NH−), 7.32−6.70 (m, 7H, Ar−H), 5.89 (s, 1H, C8a−H), 4.18−3.68 (m, 2H, C2−H_2), 2.39−2.05 (m, 2H, C3−H_2), 2.31 (s, 3H, Ar−CH_3), and 1.56 (s, 3H, C3a−CH_3) ppm; CI-MS (CH_4), *m/z* 326 (MH^+), 193 and 134. HR-MS *m/z* calcd for $C_{19}H_{20}NO_4$: 326.1392. Found: 326.1402. Anal. ($C_{19}H_{19}N\ O_4 \cdot {}^3/_8H_2O$) C, H. N: calcd 4.31; found 3.71.

Product 10: ^{1}H NMR ($CDCl_3$) δ 7.87 (s, br, 1H, −NH−), 7.33−6.70 (m, 7H, Ar−H), 5.79 (d, J = 1.80 Hz, 1H, C2−H), 4.22, 3.79 (AB, J_{gem} = 6.84 Hz, 2H, C4−H_2), 2.37−2.01 (m, 2H, C10−H_2), 2.31 (s, 3H, Ar−CH_3), and 1.51 (s, 3H, C5−CH_3) ppm; CI-MS(CH_4), *m/z* 326 (MH^+) 193 and 134. HR-MS *m/z* calcd for $C_{19}H_{20}NO_4$: 326.1392. Found: 326.1387. Anal. ($C_{19}H_{19}N\ O_4$) C, H. N: calcd 4.31; found 3.78.

3a-Methyl-2,3,3a,8a-tetrahydrofuro[2,3-*b*]benzofuran-5yl *N*-(4′-Isopropylphenyl)carbamate (11) and 4,5-Dihydro-2,5-methano-5-methyl-1,3-benzodioxepin-7-yl *N*-(4′-Isopropylphenyl)carbamate (12). Under a nitrogen atmosphere, two small pieces of sodium (∼1 mg per piece) were added into a solution of compounds **5** and **6** (18.0 mg, 0.094 mmol) in 5 mL of dry ether at room temperature. The mixture was stirred for 2 min, and then *p*-isopropylphenyl isocyanate (15.1 mg, 0.094 mmol) was added in a single portion. The reaction was continued for a further 45 min at room temperature, and then 3 mL of water was added and the ether layer was separated. After drying over sodium sulfate and filtering, the filtrate was subjected to evaporation to remove solvent. The resulting residue was chromatographed on a preparative TLC silica gel plate (EtOAc/hexane = 1/3) to afford separate products **11** (11.6 mg, 70.0%) and **12** (10.0 mg, 60.0%) as colorless gums.

Product 11. The gumlike material then was crystallized from the mixed solvents of EtOAc and hexane to provide cubic transparent crystals: mp 156−158 °C; ^{1}H NMR ($CDCl_3$) δ 7.31−6.71 (m, 8H, Ar−H and −HN−), 5.80 (s, 1H, C8a−H), 4.09−3.59 (m, 2H, C2−H_2), 2.82 (septet, J = 5.24 Hz, 1H, $-CHMe_2$), 2.19−1.96 (m, 2H, C3−H_2), 1.49 (s, 3H, C3a−CH_3), and 1.18 (d, J = 5.24 Hz, 6H, $-CHMe_2$) ppm; CI-MS(CH_4), *m/z* 354 (MH^+). HR-MS *m/z*: calcd for $C_{21}H_{24}NO_4$: 354.1705. Found: 354.1716. Anal. ($C_{21}H_{23}N\ O_4$) C. H: calcd 6.56; found 7.05. N: calcd 3.96; found 4.56. **Product 12.** The gumlike material was crystallized from mixed solvents of EtOAc and

hexane to afford needle-like transparent crystals: mp 149−150 °C; ^{1}H NMR ($CDCl_3$) δ 7.30−6.72 (m, 8H, Ar−H and −HN−), 5.71 (d, J = 1.80 Hz, 1H, C2−H), 4.17, 3.70 (AB, J_{gem} = 5.40 Hz, 2H, C4−H_2), 2.81 (septet, J = 5.22 Hz, 1H, $CHMe_2$), 2.19−1.94 (m, 2H, C10−H_2), 1.48 (s, 3H, C5−CH_3), and 1.19 (d, J = 5.22 Hz, 6H, CH_3CCH_3) ppm; CI-MS (CH_4), *m/z* 354 (MH^+); HR-MS *m/z* calcd for $C_{21}H_{24}NO_4$: 354.1705. Found: 354.1695. Anal. ($C_{21}H_{23}N\ O_4 \cdot {}^3/_4H_2O$) C, H, N.

X-ray Crystallography. Single-Crystal X-ray Analysis of 11 and 12. A colorless crystal of **11** with dimensions 0.22 mm × 0.26 mm × 0.26 mm[36b] was mounted on glass fiber using a small amount of epoxy. A colorless crystal of **12** was mounted in an identical manner and had the dimensions of 0.18 mm × 0.21 mm × 0.40 mm.[36b] Data for compounds **11** and **12** were collected on a Bruker three-circle platform diffractometer equipped with a SMART 6000 CCD detector. Both crystals were irradiated using a rotating anode Cu Kα source (λ = 1.541 78) with incident beam Göbel mirrors. Data collection was performed, and the unit cell was initially refined by using SMART [version 5.625].[36a]

Compounds **11** and **12** were both nonmerohedral twins with the approximate ratios of 70:30 and 75:25, respectively. This required an orientation matrix to be found for each component. This was done, and the data reduction for both components was performed using SAINT [verson 6.36A][36b] and XPREP [verson 6.12].[36c] Corrections were applied for Lorentz polarization and absorption effects using TWINABS [version 1.05].[36d] Each structure was solved and refined with the aid of the SHELXTL-plus [verson 6.10] system of programs.[36e] The full-matrix least-squares refinement on F^2 included atomic coordinates and anisotropic thermal parameters for all non-H atoms. The H atoms were included using a riding model. The final refinements included the structure factors from both twin components.

The two racemates of compound **11** occupy the same crystallographic site in the lattice. This appears as a superposition of the two molecules resulting in a disorder around C3A and C8A. The disorder was modeled with a 50:50 ratio of occupancies between the racemates.

Quantitation of Anticholinesterase Activity. The action of compounds **7**−**14** to inhibit the ability of freshly prepared human AChE and BChE to enzymatically degrade their respective specific substrates, acetyl(β-methyl)thiocholine and *s*-butyrylthiocholine (0.5 mmol/L) (Sigma Chemical Co., St. Louis, MO), was quantified.[3,7,16−19,23] Samples of AChE and BChE were derived from whole red blood cells and plasma, respectively. Compounds were dissolved in Tween-80/EtOH 3:1 (v/v; <150 μL total volume) and were diluted in 0.1 M Na_3PO_4 buffer (pH 8.0) in half-log concentrations to provide a final concentration range that spanned 0.3 nM to 30 μM. Tween-80/EtOH was diluted to in excess of 1 in 5000, and no inhibitory action on either AChE or BChE was detected in separate prior experiments.

For the preparation of BChE, freshly collected blood was centrifuged (10000*g*, 10 min, 4 °C) and plasma was removed and diluted 1:125 with 0.1 M Na_3PO_4 buffer (pH 7.4). For AChE preparation, whole red blood cells were washed five times in isotonic saline, lysed in 9 volumes of 0.1 M Na_3PO_4 buffer (pH 7.4) containing 0.5% Triton-X (Sigma) and then were diluted with an additional 19 volumes of buffer to a final dilution of 1:200.

Analysis of anticholinesterase activity was undertaken by utilizing a 25 μL sample of each enzyme preparation and was undertaken at their optimal working pH, 8.0, in 0.1 M Na_3PO_4 buffer (0.75 mL total volume). Compounds were preincubated with enzymes (30 min at room temperature) and then were incubated with their respective substrates and with 5,5′-dithiobis-2-nitrobenzoic acid (25 min, 37° C). Substrate−enzyme interaction was immediately halted by the addition of excess enzyme inhibitor (physostigmine 1×10^{-5} M), and production of a yellow thionitrobenzoate anion was then measured by spectrophotometer at 412 nm wavelength. To correct for nonspecific substrate hydrolysis, aliquots were co-incubated under conditions of absolute enzyme inhibition (by the addition of 1×10^{-5} M physostigmine (**2**)), and the associated alteration in absorbance was subtracted from that observed through the concentration range of each test compound. Each agent was analyzed on four separate occasions and assayed alongside physostigmine (**2**) as a control and external standard whose activity we have previously reported.[3,7,16−19,23] The enzyme activity at each concentration of test compound was expressed as a percent of the activity in the absence of compound. This was transformed into a logit format (logit = ln{(% activity)/[100 − (% activity)}) and then was plotted as a function of its log concentration. Inhibitory activity was calculated as an IC_{50}, defined as the concentration of compound (nM) required to inhibit 50% of enzymatic activity and determined from a correlation between log concentration and logit activity. Only results obtained from correlation coefficients of $r^2 > -0.98$ were considered acceptable. Studies that did not obtain this threshold were repeated.

Quantitation of Proliferation and Action on β-Amyloid Precursor Protein (APP) Levels. Human neuroblastoma SK-N-SH cells were seeded onto 60 mm culture plates supplemented with 10% FBS (Gibco/InVitrogen) in MEM Eagle (Mediatech/Cellgro) and grown to 80% of confluence. Compounds **9** and **10** were dissolved in 100% DMSO to a concentration of 0.01 M and were further diluted with media to obtain final treatment levels of 10 and 30 μM. A final sample size of 20 plates and a treatment/control number of 4 per group were utilized as a study design: vehicle control (0.3% DMSO) and **9** and **10** both at 10 and 30μM. At the initiation of the study, low serum media (0.05% FBS in MEM Eagle) and compound or control vehicle was added to cells. At 48 h thereafter, the conditioned media and cell pellet were collected for analysis. Specifically, (i) a MTT assay was performed on live cells to measure cell viability at the 48 h harvest time (n = 4). (ii) Levels of lactate dehydrogenase (LDH) were assayed in the conditioned media for assessment of cellular toxicity (n = 4).[37,38] (iii) A small aliquot of cells from each group was removed and stored on ice for cell counting by the trypan blue method (n = 1) as a secondary measure of cellular viability, and (iv) conditioned media samples were subjected to Western blot analysis using a primary antibody against total secreted APP (sAPP). This was undertaken on a 10% SDS−PAGE gel, and samples (n = 4 per treatment or control group) were loaded at equal protein (30 μg), based on the Bradford microassay protein estimation. Primary antibodies were 22C11 (APP) at 1:500 dilution and B-actin at 1:2000 dilution, both probed for 3 h at room temperature.

Computer-Aided Molecular Modeling. Computer-aided molecular modeling was undertaken using Sybyl [version 6.9 (Tripos Inc.)]. The atomic coordinates of the carbamoylated AChE, obtained from the Protein Data Bank (PDB entry: 1oce),[30] were used for docking studies. All hydrogens were added with the biopolymer module after removing the crystallographic water and the carbamoylated part, and atomic positions were refined by energy minimization. The active site residue Phe 330 was replaced with Tyr with similar conformation to match the active site of human AChE.[39] Thereafter, compound **9** was manually docked with Ser 200 and residues of the oxyanion hole as the guide. The active site (residues within 10 Å radius of compound **9**) of the complex was energy-minimized by the conjugate gradient method with a distance-dependent dielectric constant of 4.

Acknowledgment. The authors are grateful to the Medicinal Chemistry Section, National Institute on Drug Abuse, NIH, for use of chemical characterization and molecular modeling equipment. S.S.K. was supported by a National Institutes of Health Visiting Fellowship.

Supporting Information Available: Elemental analysis, NMR, and crystallographic data. This material is available free of charge via the Internet at http://pubs.acs.org.

References

(1) (a) Marion, L. *Alkaloids* **1952**, *2*, 438. (b) Coxworth, E. *Alkaloids* **1965**, *8*, 27. (c) Robinson, B. *Alkaloids* **1967**, *10*, 383. (d) Robinson, B. *Alkaloids* **1971**, *13*, 213. (e) Takano, S.; Ogasawara, K. *Alkaloids* **1989**, *36*, 889.

(2) Dale, F. J.; Robinson, B. The synthesis and anti-acetylcholinesterase activities of (+)-physostigmine and (+)-physovenine. *J. Pharm. Pharmacol.* **1970**, *22*, 889−896.

(3) Yu, Q. S.; Liu, C.; Brzostowska, M.; Chrisey, L.; Brossi, A.; Greig, N. H.; et al. Physovenines: Efficient Synthesis of (−)- and (+)-Physovenine and Synthesis of Carbamate Analogues of (−)-Physovenine. Anticholinesterase Activity and Analgesic Properties of Optically Active Physovenines. *Helv. Chim. Acta* **1991**, *74*, 761−766.

(4) Lahiri, D. K.; Farlow, M. R.; Sambamurti, K.; Greig, N. H.; Giacobini, E.; Schneider, L. S. A critical analysis of new molecular targets and strategies for drug developments in Alzheimer's disease. *Curr. Drug Targets* **2003**, *4*, 97−112.

(5) Kaplan, D.; Barak, D.; Ordentlich, A.; Kronman, C.; Velan, B.; Shafferman, A. Is aromaticity essential for trapping the catalytic histidine 447 in human acetylcholinesterase? *Biochemistry* **2004**, *43*, 3129−36.

(6) Soreq, H.; Zakut, H. *Human Cholinesterases and Anticholinesterases*; Academic Press: New York, 1993.

(7) Sussman, J. L.; Harel, M.; Frolow, F.; Oefner, C.; Goldman, A.; Toker, L.; Silman, I. Atomic Structure of Acetylcholineesterase from *Torpedo californica*: A Prototypic Acetylcholine-Binding Protein. *Science* **1991**, *253*, 872−879.

(8) Data were calculated by using software Pallas 3.0 produced by CompuDrug International Inc., 705 Grandniew Drive, South San Francisco, CA 94708.

(9) He, X. S.; Greig, N. H.; Broosi, A. Thiaphysovenine and carbamate analogues: a new class of potent inhibitors of cholinesterase. A. *Med. Chem. Res*. **1992**, *2*, 229−237.

(10) Büchi, G.; Weinreb, M. Total syntheses of aflatoxin M_1 and G_1 and an improved synthesis of aflatoxin B_1. *J. Am. Chem. Soc*. **1971**, *93*, 746−752.

(11) Civitello, E. R.; Rapoport, H. Synthesis of the Enantiomeric Furobenzofurans, Late Precursors for the Synthesis of (+)- and (−)-Aflatoxins B_1, B_2, G_1 and G_2. *J. Org. Chem.* **1994**, *59*, 3775−3782.

(12) Graybill, T. L.; Casillas, E. G.; Pal, K.; Townsend, C. A. Silyl Triflate-Mediated Ring-Closure and Rearrangement in the Synthesis of Potential Bisfuran-Containing Intermediates of Aflatoxin Biosynthesis. *J. Am.Chem. Soc*. **1999**, *121*, 7729−7746.

(13) Ozaki, Y.; Quan, Z. S.; Watabe, K. (née Okamura); Kim, S. W. Synthesis of 5-hydroxyoxaindan-2-ones and indol-5-ols from 1,4-cyclohexanedione. *Heterocycles* **1999**, *51*, 727−731.

(14) Harley-Mason, J.; Jackson, A. H. Hydroxytryptamine. Part II. A New Synthesis of Physostigmine. *J. Chem. Soc.* **1954**, 3651−3654.

(15) Shaw, K. T. Y.; Rogers, J.; Utsuki, T.; Yu, Q. S.; Sambamurti, K.; Brossi, A.; Ge, Y. W.; Lahiri, D. K.; Greig, N. H. Phenserine regulates traslation of β-amyloid precursor protein mRNA by a putative interleukin-1 responsive element: a novel target for drug development. *Proc. Natl. Acad. Sci. U.S.A.* **2001**, *98*, 7605−7610.

(16) Sambamurti, K.; Greig, N. H.; Lahiri, D. K. Advances in the cellular and molecular biology of the beta-amyloid protein in Alzheimer's disease. *NeuroMol. Med.* **2002**, *1*, 1−31.

(17) Pei, X. F.; Bi, S.; Brossi, A. Reduction of oxindoles with sodium bis(2-methoxyethoxy) aluminum hydride, a novel reducing agent. *Heterocycles* **1994**, *39*, 357−360.

(18) Brzostowska, M.; He, X. S.; Greig, N. H.; Rapoport, S.; Brossi, A. Phenylcarbamates of (−)-Eceroline and (−)-Physovenol: Selective Inhibition of Acetyl and/or Butyrylcholinesterases by Phenylcarbamates. *Med. Chem. Res.* **1992**, *2*, 238−246.

(19) Yu, Q. S.; Atack, J. A.; Rapoport, S.; Brossi, A. Carbamate analogues of (−)-physostigmine: in vitro inhibition of acetyl- and butyrylcholinesterase. *FEBS Lett.* **1988**, *234*, 127−130.

(20) Atack, J. R.; Yu, Q. S.; Soncrant, T. T.; Brossi, A.; Rapoport, S. Comparative Inhibitory Effects if Variou Physostigmine Analogs against Acetyl- and Butyrylcholinesterases. *J. Pharmacol. Exp. Ther.* **1989**, *249*, 194−249.

(21) Pei, X. F.; Greig, N. N.; Bi, S.; Broosi, A.; Toome, V. Inhibition of human acetylcholinesterase by unnatural (+)-(3a*R*)-N1-norphysostigmine and arylcarbamate analogues. *Med. Chem. Res.* **1995**, *5*, 265−270.

(22) Greig, N. H.; DeMicheli, E.; Utsuki, T.; Holloway, H. W.; Yu, Q. S.; Perry, T. A.; Brossi, A.; Deutsch, J.; Ingram, D. K.; Lahiri, D. K.; Soncrant, T. The experimental Alzheimer drug phenserine: pharmacodynamics and kinetics in the rat. *Acta Neurol. Scand*. **2000**, *102*, 74−84.

(23) Yu, Q. S.; Holloway, H. W.; Flippen-Anderson, J. L.; Hoffman, B.; Brossi, A.; Greig, N. H. Methyl analogues of the experimental Alzheimer drug phenserine: synthesis and structure/activity relationship for acetyl- and butyrylcholinesterase inhibitory action. *J. Med. Chem.* **2001**, *44*, 4062−4071.

(24) Giacobini, E. *Cholinesterase and Cholinesterase Inhibitors*; Martin Dunitz: London, 2000.

(25) Giacobini, E. *Butyrylcholinesterase, Its Function and Inhibitors*; Martin Dunitz: London, 2003.

(26) Yu, Q. S.; Luo, W.; Holloway, H. W.; Utsuki, T.; Perry, T. A.; Lahiri, D. K.; Greig, N. H.; Brossi, A. Racemic N^1-norphenserine and its enatiomers: unpredicted inhibition of human acetyl- and butylylcholinesterase and β-amyloid precursor protein *in vitro*. *Heterocycles* **2003**, *619*, 529−539.

(27) Nolte, H. J.; Rosenberry, T. L.; Neumann, E. Effective Charge on Acetylcholinesterase Active Sites Determined from the Ionic Strength Dependence of Association Rate Constants with Cationic Ligands. *Biochemistry* **1980**, *19*, 3705−3711.

(28) Ripoll, D. R.; Faerman, C. H.; Axelsen, P. H.; Silman, I.; Sussman, J. L. An Electrostatic Mechanism for Substrate Guidance down the Aromatic Gorge of Acetylcholinesterase. *Proc. Natl. Acad. Sci. U.S.A.* **1993**, *90*, 5128−5132.

(29) Tan, R. C.; Truong, T. N.; McCammon, J. A.; Sussman, J. L. Acetylcholinesterase: Electrostatic Steering Increases the Rate of Ligand Binding. *Biochemistry* **1993**, *32*, 401−403.

(30) Bartolucci, C.; Perola, E.; Cellai, L.; Brufani, M.; Lamba, D. "Back Door" Opening Implied by the Crystal Structure of Carbamoylated Acetylcholinesterase. *Biochemistry* **1999**, *38*, 5714−5719.

(31) Gilson, M. K.; Straatsma, J. A.; McCammon, J. A.; Ripoll, D. R.; Faerman, C. H.; Axelsen, P. H.; Silman, I.; Sussman, J. L. Open "Back Door" in a Molecular Dynamics Simulation of Acetylcholinesterase. *Science* **1994**, *263*, 1276−1278.

(32) Koellner, G.; Steiner, T.; Millard, C. B.; Silman, I.; Sussman, J. L. A Neutral Molecule in a Cation-Binding Site: Specific Binding of a PEG-SH to Acetylcholinesterase from *Torpedo californica*. *J. Mol. Biol.* **2002**, *320*, 721−725.

(33) Pei, X. F.; Yu, Q. S.; Holloway, H. W.; Brossi, A.; Greig, N. H. Syntheses and biological evaluation of ring-C opened analogues of the cholinesterase inhibitors physostigmine, phenserine and cymserine. *Med. Chem. Res.* **1999**, *9*, 50−60.

(34) Lahiri, D. K.; Alley, M.; Farlow, H.; Rogers, J. T.; Greig, N. H. Physostigmine and its analogue phenserine have different effects of Alzheimer's amyloid-beta precursor protein. In *Progress in Alzheimer's and Parkinson's Disease*; Hanin, I., Fisher, A., Eds., in press.

(35) Maloney, B.; Ge, Y.; Greig, N. H.; Lahiri, D. K. Characterization of the 5′-untranslated region of APP mRNA: implications in drug development for Alzheimer's disease. *FASEB J*. **2004**, *18*, 1288−1290.

(36) Computer software used for X-ray crystallography: (a) . *SMART*, version 5.625; Bruker AXS Inc.: Madison, WI, 2001. (b) *SAINT*, version 6.36A; Bruker AXS Inc.: Madison, WI, 2002. (c) *XPREP*, version 6.12; Bruker AXS Inc.: Madison, WI, 2001. (d) *TWINABS*, version 1.05; Bruker AXS Inc.: Madison, WI, 2003. (e) *SHELXTL*, version 6.10; Bruker AXS Inc.; Madison, WI, 2000.

(37) Lahiri, D. K.; Farlow, M. R.; Sambamurti, K. The Secretion of Amyloid-beta Peptides Is Inhibited in Tacrine-Treated Human Neuroblastoma Cells. *Mol. Brain Res.* **1998**, *62*, 131−140.

(38) Zhu, X.; Yu, Q. S.; Cutler, R. G.; Culmsee, C.; Holloway, H. W.; Mattson, M. P.; Greig, N. H. Novel p53 inhibitors with neuroprotective action: syntheses and pharmacological evaluation of 2-imino-2,3,4,5,6,7-hexahydrobenzothiazole and 2-imino-2,3,4,5,6,7-hexahydrobenzoxazole derivatives. *J. Med. Chem*. **2002**, *45*, 5090−5097.

(39) Yamamoto, Y.; Ishihara, Y.; Kuntz, I. D. Docking Analysis of a Series of Benzylamino Acetylcholinesterase Inhibitors with a Phthalimide, Benzoyl, or Indanone Moiety. *J. Med. Chem.* **1994**, *37*, 3141−3153.

(40) Enz, A.; Amstutz, R.; Boddeke, H.; Gmelin, G.; Malanowski, J. Brain selective inhibition of acetylcholinesterase: a novel approach to therapy in Alzheimer's disease. *Prog. Brain Res*. **1993**, *98*, 431−438.

JM049309+